Published in final edited form as:
Dev Biol. 2009 June 15; 330(2): 305–317. doi:10.1016/j.ydbio.2009.03.028.

Sonic hedgehog maintains proliferation in secondary heart field progenitors and is required for normal arterial pole formation

Laura A. Dyer[1] and **Margaret L. Kirby**[1,2,*]

[1] Department of Cell Biology, Duke University, Durham, NC 27710

[2] Department of Pediatrics, Duke University, Durham, NC 27710

Abstract

The Sonic hedgehog (Shh)-null mouse was initially described as a phenotypic mimic of Tetralogy of Fallot with pulmonary atresia (Washington-Smoak et al, 2005); however, subsequent reports describe only a single outflow tract, leaving the phenotype and its developmental mechanism unclear. We hypothesized that the phenotype that occurs in response to Shh knockdown is pulmonary atresia and is directly related to the abnormal development of the secondary heart field. We found that Shh was expressed by the pharyngeal endoderm adjacent to the secondary heart field and that its receptor Ptc2 was expressed in a gradient in the secondary heart field, with the most robust expression in the caudal secondary heart field, closest to the Shh expression. In vitro culture of secondary heart field with the hedgehog inhibitor cyclopamine significantly reduced proliferation. In ovo, cyclopamine treatment before the secondary heart field adds to the outflow tract reduced proliferation only in the caudal secondary heart field, which coincided with the region of high Ptc2 expression. After outflow tract septation should occur, embryos treated with cyclopamine exhibited pulmonary atresia, pulmonary stenosis, and persistent truncus arteriosus. Cardiac neural crest-derived cells, which form the outflow tract septum, migrated into the outflow tract and formed a septum. However, this septum divided the outflow tract into two unequal sized vessels and effectively closed off the pulmonary outlet. These experiments show that Shh is necessary for secondary heart field proliferation, which is required for normal pulmonary trunk formation, and that embryos with pulmonary atresia have an outflow tract septum.

Keywords

Secondary heart field; arterial pole; heart; Sonic hedgehog; Tetralogy of Fallot

Introduction

In the bilateral cardiac fields, Nxk2.5 expression is maintained in the second heart field after the first heart field has down-regulated Nxk2.5 and formed the initial heart tube (Prall et al, 2007). Within this second heart field, the secondary heart field is a specific region that is located in the pharyngeal splanchnic mesoderm caudal to the outflow tract (Waldo et al., 2001). During heart looping, the outflow tract is displaced caudally with respect to the pharyngeal arches, and

*Address for correspondence: Dr. Margaret L. Kirby, DUMC, Box 3179, Durham, NC 27710, Phone: 919-668-1598; Fax: 919-668-1599; mlkirby@duke.edu.

the secondary heart field cells nearest the outflow tract migrate into the outflow tract (Waldo et al., 2001).

The secondary heart field differentiates into first cardiac and then smooth muscle. Outflow tract myocardium is added over a 24-hour period in chick, spanning Hamburger Hamilton (HH) stages 14 through 18. This myocardium ultimately incorporates into the ventricles, forming the subvalvular outlets. Smooth muscle is generated between HH 18 and HH 22 and forms the tunica media at the base of the arterial trunks (Waldo et al., 2005a). The outflow tract is septated by cardiac neural crest-derived cells, forming aortic and pulmonary outlets, and the aorta subsequently becomes "wedged" between the atrioventricular valves, behind the pulmonary trunk (Kirby, 2007).

Ablation of the right secondary heart field progenitors causes defects in both the subpulmonary myocardium and the smooth muscle junction of the coronary arteries with the aorta (Ward et al., 2005). These phenotypes are consistent with the human congenital heart defect Tetralogy of Fallot.

Tetralogy of Fallot affects 9–14% of children born with congenital heart defects and affects four of every 10,000 live births each year (Rosamond et al., 2007; Hoffman and Kaplan, 2002). Several genes have been linked to Tetralogy of Fallot, including transcription factor Tbx1. The Tbx1-null mouse shows diminished proliferation in the secondary heart field and a solitary outflow vessel (Xu et al., 2004). Sonic hedgehog (Shh) is among the genes that interact with Tbx1 (Garg et al., 2001), and the Shh-null mouse also has arterial pole defects, including a phenocopy of Tetralogy of Fallot with complete pulmonary atresia (Washington-Smoak et al., 2005). Interestingly, subsequent analyses of mice lacking Shh in the pharyngeal endoderm described a single outflow tract vessel with disrupted pharyngeal arch arteries and impaired cardiac neural crest cell migration (Goddeeris et al., 2007; Goddeeris et al., 2008). The single outflow vessel was not classified. This study identified apoptosis in the pharyngeal endoderm and splanchnic mesoderm as a potential cause of these defects; however, apoptosis was evaluated at a stage that was too late to identify aberrant apoptosis specifically in the secondary heart field. As such, the arterial pole defects that occur in the absence of Shh signaling remain unidentified, and the mechanism through which these defects occur is unknown. We hypothesized that Shh specifically affected the secondary heart field.

We first determined that Shh mRNA was expressed in the pharyngeal endoderm adjacent to the secondary heart field; however, receptor and downstream target Patched 2 (Ptc2) was expressed in the secondary heart field, confirming that the secondary heart field responds to Shh signaling. Ptc2 expression formed a gradient, with lowest expression levels adjacent to the outflow tract and highest expression in the caudal secondary heart field. When secondary heart field explants were incubated with Shh inhibitor cyclopamine, proliferation was reduced. In ovo, cyclopamine reduced proliferation only in the region of the secondary heart field that showed intense Ptc2 expression. Arterial pole defects, including pulmonary atresia and stenosis, pulmonary atresia (PTA), and abnormal patterning of the aortic arch arteries, were induced in a stage-dependent manner. Importantly, cardiac neural crest-derived cells migrated into the outflow tract cushions and formed a septum in embryos with pulmonary atresia, albeit the septum appeared to close off the pulmonary outlet, leaving a single outflow vessel. In addition, coronary artery abnormalities were seen in one-third of treated embryos. These data support a role for Shh in maintaining proliferation in a subset of secondary heart field progenitors to allow an optimal number of myocardial and smooth muscle cells to migrate to the arterial pole.

Materials and methods

Embryos

Fertilized Ross Hubert chick eggs (Gallus domesticus, Pilgrim Hatchery, Siler City, NC) were incubated for 1–9 days, and Coturnix quail eggs (Coturnix coturnix, Ozark Egg Co, Stover, MO) were incubated for 1–2 days; both were maintained at 37°C and 70% humidity. Embryos were staged according to Hamburger and Hamilton (1951).

Antibodies and immunohistochemistry

The following primary antibodies were used: QCPN and MF20 (Developmental Studies Hybridoma Bank, Iowa City, IA); anti-BrdU (Roche, Indianapolis, IN); and SM22-α (Abcam, Cambridge, MA). BrdU was detected using the ABC Vectastain and avidin-biotin DAB kits (Vector Laboratory, Burlingame, CA); the other antibodies were visualized using AlexaFluor 488 or AlexaFluor 568 (Molecular Probes, Carlsbad, CA). QCPN was used as described by Waldo et al. (1998); all other antibodies followed the protocol described by Waldo et al. (1996).

In situ hybridization

Shh and Ptc2 plasmids were generously provided by Cliff Tabin. Embryos were harvested at HH 15-16 in DEPC-treated 4% paraformaldehyde. In situ hybridization was carried out as described by Wilkinson (1992). Control and drug-treated embryos were developed in alkaline-phosphatase detection solution for the same length of time. After whole mount photography, embryos were paraffin embedded and sectioned at 10 μm. Some sections were counterstained with eosin.

Secondary heart field isolation

At HH 14, eggs were windowed, and 1.5 μl of 0.25 μM DiI (Molecular Probes) was pipetted into the pericardial cavity. After the dye penetrated the outer cell layer, the splanchnic mesoderm and underlying ventral pharyngeal endoderm between the outflow and inflow tracts were removed. To separate the splanchnic mesoderm comprising the secondary heart field from the underlying endoderm, the tissue was digested in 0.25% trypsin and 2.5% pancreatin (1:1) for 5 minutes. Isolated secondary heart field mesoderms were identified using DiI fluorescence and placed in 10% fetal bovine serum in Liebovitz medium with varying concentrations of cyclopamine (Sigma, St. Louis, MO). These explants express heart field marker Isl1 (R. Subramanian, personal communication) and will differentiate into both myocardium and smooth muscle.

In ovo cyclopamine treatment

Eggs were windowed, and 10 μl of cyclopamine (0.6–1.0 μg/μl) or PBS (control) was pipetted onto the embryo; eggs were sealed with tape and incubated. Unless stated otherwise, embryos were treated at HH 14. Stock cyclopamine was dissolved in 95% EtOH and diluted with PBS. Ninety percent of the drugged embryos survived to HH 35 (10 of 11 embryos treated with 0.6 μg/μl, and 9 of 10 embryos treated with 0.8 μg/μl cyclopamine). Shell-less culture (Ward et al., 2005) was initially used but yielded lower survival (4 of 12 embryos treated with 0.6 μg/μl, 4 of 10 embryos treated with 0.8 μg/μl, and 2 of 4 embryos treated with 1.0 μg/μl survived to HH 35). Embryos incubated in shell-less culture exhibited the same phenotypes as those treated in ovo and have been included in the analysis. Three embryos (two shell-less culture and one in ovo) that died just prior to collection and had good tissue preservation were included, so 32 treated embryos were collected. Embryos were harvested, photographed, fixed in 10% formalin overnight at 4°C, paraffin embedded, sectioned, and stained with hematoxylin and

eosin. Because embryos treated at HH 14 with 1.0 μg/μl cyclopamine that survived to HH 35 were generally unhealthy, they were excluded from the detailed section analysis.

Quantitative reverse transcription PCR (qRT-PCR)

To confirm that cyclopamine inhibits the hedgehog pathway in ovo, secondary heart field explants were excised from HH 16 control and drug-treated embryos. mRNA was then isolated using the Qiagen RNeasy kit (Qiagen, Valencia, CA). cDNA was reverse transcribed by incubating 30 μl mRNA, 2 μl random hexamer primers, and 1 μl dNTPs for 5 minutes at 72° C; then adding 9.5 μl 5× reaction buffer, 3 μl 0.1M DTT, and 1 μl RNase inhibitor and incubating for 2 minutes at room temperature; and finally adding 1 μl superscript II and incubating for 2 hours at 37°C. cDNA was stored at −20°C.

For qRT-PCR, primers were designed for Ptc1, Ptc2, and housekeeping gene HPRT (Table 1). Primer efficiency was tested over a linear range of starting cDNA (0.5–500 ng) and calculated according to Pfaffl (2004). The PCR mix consisted of 100 ng cDNA, SybrGreen, and 1 μl of each primer (10 nM each) in a total of 25 μl. cDNA was amplified using the following cycle parameters: 95°C for 2 minutes; 40 cycles of 94°C for 30 seconds, 56°C for 20 seconds, and 72°C for 30 seconds; and 72°C for 10 minutes. Relative expression was calculated based on the ratio of target gene ΔCP to the reference gene ΔCP, adjusted for primer efficiency (Pfaffl, 2004).

Secondary heart field migration

Secondary heart field explants were placed on a warmed stage (LiveCell, Westminster, MD) maintained at 37°C. To quantify cell migration, a Nikon Eclipse TE2000-U microscope and MetaMorph software were used to photograph the explants at the beginning and end of a 16-hour period. At least six explants per treatment were recorded, and relative migration indices were calculated based on Epstein et al. (2000). The difference in explant area between the end and the beginning of the 16-hour period was calculated and normalized by dividing this difference by the explant perimeter at the end of the 16-hour period (see Fig. 2A, B for an example). This normalization allowed for comparisons to be made between explants of varying sizes. Statistical significance was determined using unpaired Student's t-test with equal variances.

Secondary heart field proliferation

To measure proliferation in the secondary heart field, both secondary heart field explants and whole embryos were treated with BrdU as described in Waldo et al. (2001). Secondary heart field explants were treated with BrdU 24 hours post-dissection, fixed in methanol, immunolabeled for BrdU and myocardium (using MF20), and counterstained with DAPI (Molecular Probes) to visualize nuclei. To determine the rate of proliferation and the percentage of myocardial differentiation, at least 300 cells within the monolayer that migrated away from each explant were counted. Explants with less than 300 migratory cells were excluded from further analysis. A minimum of six explants per dose was counted to calculate statistical significance, which was determined using unpaired Student's t-test with equal variances.

To determine whether proliferation differences also occurred in ovo, embryos were treated with cyclopamine or PBS at HH 14, and mitotic indices were determined using BrdU incorporation as described in Waldo et al. (2001). Sections were co-labeled with MF20 and DAPI. Proliferating cells within the first 80 secondary heart field cells, starting at the junction of the outflow tract and moving caudally through the secondary heart field, were counted. Alternating 10-μm sections were counted in 10-cell increments, and only embryos with a secondary heart field spanning 110 μm were analyzed. The average proliferation per 10-cell increment was calculated in each embryo, and at least three embryos were counted per

treatment. Statistical significance was determined using unpaired Student's t-test with equal variances.

India ink injections

To determine whether arch artery patterning was normal, pharyngeal arch arteries were visualized in control and cyclopamine-treated embryos between HH 17 and 29 by injecting India ink into a vitelline vein. Ink-injected embryos were harvested, fixed overnight at 4°C in Carnoy's, and cleared in a 1:1 methylsalicylate:benzylbenzoate solution. To further characterize the arch artery patterns, HH 29 embryos were washed in toluene for paraffin embedding, and sections were counterstained with eosin.

Quail-chick chimeras

Quail-chick chimeras were made as described in Kirby (1988) to observe whether cardiac neural crest-derived cells migrated into the outflow tract and formed a septum after cyclopamine treatment. Host eggs were sealed with tape and reincubated to HH 14, when they were treated with 0.8 μg/μl cyclopamine or PBS and reincubated to either HH 23-24 or HH 35. Embryos harvested at HH 23-24 were fixed in 4% paraformaldehyde at 4°C overnight, and embryos harvested at HH 35 were fixed in methacarn at 4°C overnight. All embryos were paraffin embedded, sectioned, and labeled with QCPN to recognize quail cells, either the Vector Apoptag kit to recognize apoptotic cells (HH 23-24) or muscle markers (HH 35), and DAPI.

Results

Shh expression pattern

Previous work has shown that Shh is expressed in the cerebellum, the foregut, and the pharyngeal arches (Ingham and McMahon, 2001; Moore-Scott and Manley, 2005); however, it is unclear whether Shh is expressed within or near the secondary heart field. We found Shh mRNA expression in whole mount embryos in the caudal boundaries of pharyngeal arches two and three and the foregut (Fig. 1A). At HH 15, foregut expression was specific to the pharyngeal endoderm and was most robust in the ventral midline endoderm caudal to the outflow tract (Fig. 1A′). Lateral to the midline, expression was reduced (data not shown). Desert and Indian hedgehogs were not detected in murine secondary heart field and pharyngeal endoderm explants by microarray analysis and were not analyzed further (Dyer and Kirby, unpublished). The ability of the secondary heart field to respond to Shh signaling was determined using in situ hybridization to localize Shh receptor and downstream target Ptc2. In whole mount, Ptc2 expression was similar to that of Shh mRNA in the caudal boundaries of the pharyngeal arches and was also present in the pharynx (Fig. 1B). In addition, Ptc2 was specifically localized to the secondary heart field (Fig. 1B′). No expression was seen within the pharyngeal endoderm. These expression patterns confirm that the secondary heart field responds to Shh signaling. In addition, treating embryos with cyclopamine abolished Ptc2 expression in the secondary heart field and the pharyngeal arches (Fig. 1C, C′). Quantifying this decrease in excised HH 16 secondary heart fields using qRT-PCR confirmed that both Ptc1 and Ptc2 were significantly decreased by nearly 10-fold ($p<0.001$ for both receptors, Student's t-test with unequal variances, Fig. 1D).

Response of secondary heart field to hedgehog inhibitor cyclopamine in vitro

To assess the effect of Shh on secondary heart field progenitors, secondary heart field mesoderm was separated from Shh-expressing pharyngeal endoderm and treated with cyclopamine. Explants were dissected from embryos at HH 14, which coincides with the onset of the myocardial addition to the outflow tract. Over a 16-hour period, migration was reduced

by 20% in cyclopamine-treated embryos ($p<0.05$, Fig. 2F). To determine secondary heart field proliferation, the mitotic index was measured by BrdU incorporation 24 hours post-dissection. After cyclopamine treatment, secondary heart field proliferation was decreased by as much as 75% compared to control explants ($p<0.0001$, Fig. 2E). Only migration and proliferation showed a dose-dependent response to cyclopamine. Myocardial differentiation normally begins around 48 hours after culture, and no alteration in differentiation was observed. Together, these data show that inhibiting hedgehog signaling primarily decreases proliferation, slightly decreases migration, and does not affect myocardial differentiation.

Cyclopamine disrupts secondary heart field proliferation in ovo

To determine whether the distinct effect of cyclopamine on secondary heart field proliferation in vitro also occurs in ovo, embryos were treated with cyclopamine at HH 14, when the secondary heart field progenitors begin to add myocardium to the outflow tract. Treated and control embryos were initially collected at HH 16 to analyze secondary heart field proliferation. Caudal secondary heart field cells were highly proliferative (Fig. 3B). As the cells migrated into the outflow tract, they began to differentiate and elongate, and proliferation decreased by nearly 50% as the cells migrated away from the Shh-producing pharyngeal endoderm (Fig. 3A, B). Upon reaching the myocardial outflow tract, proliferation nearly ceased (Fig. 3B). In cyclopamine-treated embryos, proliferation was visibly reduced in the cells previously found to express high Ptc2 levels in the secondary heart field (Fig. 3C). Proliferation was unchanged in the cranial-most secondary heart field, which is further away from both the pharyngeal Shh source and the region of secondary heart field that expresses Ptc2.

To determine when this proliferation decrease occurs, embryos were analyzed from HH 15 to 18. In addition, to determine whether there is a proliferation gradient that correlates with the Ptc2 expression gradient, proliferation was quantified by counting proliferating secondary heart field cells starting at the myocardium and moving caudally in 10-cell increments. At HH 15, proliferation was present throughout the secondary heart field and was more robust in the caudal portion. In treated embryos, which had been exposed to cyclopamine for six hours, no change in proliferation was observed with respect to the control embryos (Fig. 3A). However, at HH 16 and 17, proliferation did not increase in the more caudal 30 cells after cyclopamine treatment (Fig. 3A, $p<0.01$) and was almost half of that which was observed in control embryos. No significant change in proliferation was seen within the cranial-most 50 cells of cyclopamine-treated embryos as compared to control embryos; this region corresponds with the lowest Ptc2 expression (see Fig. 1B). The highly proliferative region correlates with strong Ptc2 expression, suggesting that Shh signaling is required to maintain proliferation. Finally, no proliferation changes were observed at HH 18 after cyclopamine treatment, which corresponds to when Ptc2 expression appears to decrease (Supplementary Figure 1). Together, these data show that cyclopamine requires more than six hours to reduce proliferation and that this reduction is lost within 24 hours of exposure.

To determine whether decreased proliferation was accompanied by increased cell death, apoptosis was analyzed in the secondary heart field at HH 16. While an occasional cell in the secondary heart field was apoptotic, cyclopamine treatment did not induce secondary heart field apoptosis (Supplementary Figure 2).

Cyclopamine induces pulmonary atresia and stenosis

Abnormal proliferation in secondary heart field progenitors has been linked to arterial pole defects in other models (Hutson et al., 2005; Waldo et al., 2005b; Xu et al., 2004), suggesting that cyclopamine treatment may result in arterial pole defects later in development. Because the secondary heart field contributes myocardium early, at HH 14, and smooth muscle later, at HH 18, embryos were treated at both stages and allowed to develop to HH 35. Seventy-eight

percent of hearts treated at HH 14 had a single outflow vessel (n=32, Fig. 4) with anomalous great arteries. In chick, the bilaterally symmetrical pharyngeal arch arteries remodel into a right-sided aorta, giving rise to a right and left brachiocephalic artery, and a left and right ductus arteriosus. Cyclopamine-treated embryos exhibited a range of remodeling defects, with two to four vessels branching off the single outflow vessel; the brachiocephalic arteries were identifiable, and the extra vessels were likely abnormally persistent pharyngeal arch arteries. The origin of the brachiocephalic arteries (derived from pharyngeal arch artery 3) was shifted to the right side of the outflow vessel, giving a twisted appearance. In addition, disrupting Shh at HH 14 resulted in peripheral edema of varying severity (11 of 32 treated embryos); occasionally, the right eye was small (n=3), or the forelimbs were truncated (n=8).

Disruption of Shh at HH 18 (n=3) with the highest dose of cyclopamine (1.0 μg/μl) resulted only in mild edema (n=1) and limb defects (n=2); embryos looked normal, and no gross heart abnormalities were observed. Because treatment at HH 18 resulted in normal embryos, embryos were treated at additional stages to determine when they were most sensitive to Shh signaling. Embryos treated before HH 14 had a high incidence of lethality (33% of embryos treated at HH 12-13 survived to HH 34); all surviving embryos had a single outflow vessel (Supplementary Table 1). Embryos treated at HH 15 and 16 had better survival to HH 35 (80% survived to HH 35) and a reduced incidence of single outflow vessels (32.5%; Supplementary Table 1).

To distinguish between PTA and pulmonary atresia in cyclopamine-treated embryos, hearts were sectioned to confirm the identity of the single outflow vessel. The distinction between PTA (a common aortic and pulmonary vessel) and pulmonary atresia (only an aortic outflow) was made in serial sections by following the origins of both the pulmonary and systemic outflows from the ventricles through the outflow vessel. The pulmonary infundibulum, which gives rise to the pulmonary outlet, was narrow (Fig. 5B) or hypoplastic below the semilunar valves in four embryos (see Table 2 for a breakdown by dosage); the pulmonary outlet was atretic at the semilunar valves in another nine embryos. Blood would have flowed from the right ventricle via a ventricular septal defect (Fig. 5B) through a single vessel with a semilunar valve; based on the atretic right ventricular outflow, these 13 embryos were confirmed to have pulmonary atresia. Pulmonary stenosis was present in two embryos, one below and the other at the semilunar valves. PTA was seen in eight embryos (Fig. 4D). PTA was distinguished from pulmonary atresia based on the position of the single outflow vessel, which was oriented over the ventricular septum, and the pulmonary infundibulum being equivalent in size to the aortic vestibule (Fig. 5C). The last two treated embryos had a single outflow vessel that could not be identified as either pulmonary atresia or PTA.

The designation of pulmonary atresia as opposed to PTA was further confirmed by identifying the number of semilunar valve leaflets and the position of the coronary arteries. The aorta and pulmonary trunks normally have three valve leaflets each. In embryos classified as having pulmonary atresia (n=13), the semilunar valve of the presumptive aorta had three leaflets in 11 embryos (5B″); one semilunar valve had two leaflets, and the number of leaflets could not be clearly defined in the remaining embryo. In embryos classified as having PTA (n=8), the single outflow vessel had between three and five semilunar valve leaflets, in agreement with Williams et al. (1999). In one embryo with three leaflets, the valve leaflets were abnormally large, and two leaflets were poorly separated.

The location of the coronary arteries was critical in designating pulmonary atresia as opposed to PTA. After cyclopamine treatment, some embryos were missing either the left or right coronary artery (n=1 for each side), and in other embryos, the coronary arteries were either abnormally large or the vascular plexus failed to coalesce into two distinct stems (n=8); these data suggest that secondary heart field-derived smooth muscle is also disrupted after

cyclopamine treatment. However, the coronary arteries that were present in embryos classified as having pulmonary atresia arose from the single outflow vessel in the normal orientation (Fig. 5B″), confirming the identity of the single vessels as aortas. In contrast, the coronary arteries penetrated the single outflow vessel of embryos with PTA approximately where they would penetrate the systemic half of the common trunk (Fig. 5C″).

In addition to these defects, 80% of the cyclopamine-treated embryos (n=30) had ventricular septal defects, whereas a ventricular septal defect was present in only one control embryo (n=13).

Embryos treated with cyclopamine before HH 14 had either pulmonary atresia (n=2) or PTA (n=1) (Supplementary Table 1). One embryo treated at HH 13 had too many coronary arteries (one in each of four valve leaflets). Embryos treated at HH 15 and 16 also exhibited both pulmonary atresia (n=1) and PTA (n=2). One embryo treated at HH 15 had poorly coalesced coronary vessels, and one embryo treated at HH 16 was missing a coronary artery. Embryos treated at HH 18 (Fig. 5D-D″) had intact ventricular septa, normally aligned aorta and pulmonary trunk outlets, and two distinct coronary arteries that penetrated the aortic wall. The secondary heart field begins providing smooth muscle to the arterial pole at HH 18. However, no coronary artery abnormalities were seen after cyclopamine treatment at this stage, which suggests that the coronary artery anomalies seen in embryos treated at HH 14 are related to the proliferation defect observed at HH 16-17.

Altogether, these defects indicate that the pulmonary outlet is particularly sensitive to secondary heart field proliferation, which is supported by hedgehog signaling. The secondary heart field can be affected between HH 12 and HH 16, although it becomes less sensitive after HH 14, and inhibiting Shh signaling at any one particular stage does not favor pulmonary atresia over PTA. However, these results do not explain the twisted brachiocephalic arteries or the persistent arch arteries, suggesting that either the cardiac neural crest-derived cells were also affected or the aortic arch arteries are also directly affected by hedgehog signaling.

Arch artery patterning

The pharyngeal arch arteries form as bilaterally symmetrical pairs as the outflow tract gathers myocardium from the secondary heart field. At HH 18, arch arteries 1-3 are open, and arch artery 4 is forming; by HH 19, the first arch artery has regressed, and arch artery 4 has lumenized. Arch arteries 5-6 begin to form at HH 20, and when arch artery 6 is patent by HH 23, arch artery 2 has regressed. Arch artery 5 is present only briefly at HH 22. Starting at HH 28, asymmetrical remodeling begins, and the left fourth arch artery closes (Hiruma and Hirakow, 1995). Once remodeling is complete, the arch arteries are referred to as the great arteries of the thorax. To follow the development of the arch arteries, we injected India ink into cyclopamine-treated embryos. Based on the different phenotypes induced by varying doses of cyclopamine, 0.6 μg/μl was selected to favor pulmonary atresia as an outcome. At HH 18, the pharyngeal arch artery pattern looked similar between control and treated embryos; however, the first arch artery had begun regressing in the control embryo (Fig. 6A), whereas it was still robust in the treated embryo (Fig. 6B). The first and second arch arteries occasionally persisted as late as HH 22-23 (data not shown). By HH22-23, the fourth and sixth arch arteries should appear (Fig. 6C), but the right fourth and sixth arch arteries developed abnormally after cyclopamine treatment (Fig. 6D). However, most ink injected-embryos at HH 29 showed the correct patterning of the great arch artery derivatives (Fig. 6F). The left fourth arch artery had apparently closed, as in the controls, leaving left arch arteries 3 (left brachiocephalic) and 6 (right ductus arteriosus) and right arch arteries 3-6 (right brachiocephalic, aortic arch, and ductus arteriosus) (75%; n=4). One treated embryo had only two great arteries present on each side, and these arteries appeared to be arteries 3 and 6 in whole mount. In all four HH 29

embryos, the arteries were longer, with kinks; despite the early abnormalities, the overall patterning appeared normal after the remodeling stage.

The HH 29 ink-injected hearts were sectioned to confirm this apparently normal cardiovascular phenotype of cyclopamine-treated embryos. In transverse sections through PBS-treated control embryos, the expected arch arteries were present; left arch artery 3 and right arch arteries 3 and 4 branched off the aortic trunk, and both left and right arch arteries 6 joined the pulmonary trunk (Fig. 7B). These two trunks were clearly separated at the level of the outflow tract valves (n=4), and the interventricular septum was intact. In cyclopamine-treated embryos, almost all right-sided arch arteries appeared normal (n=4); however, one embryo lacked both the right and left sixth arch arteries and maintained both fourth arch arteries instead. In this case, the left fourth arch artery connected to the heart where the pulmonary trunk would originate. In another embryo, a remnant of the left fourth arch artery remained, and the left and right sixth arch arteries branched off the dorsal aorta at the same level. In the remaining two embryos, the second open artery on the left side was not clearly the fourth or sixth arch artery (50%). This arch artery (designated 4/6 in Fig. 7B) connected to the heart where the pulmonary trunk should originate. While these cyclopamine-treated embryos showed a diverse range of phenotypes, most of the defects specifically affect pulmonary trunk and sixth arch artery development. These defects suggest that the cardiac neural crest, which invests and repatterns the pharyngeal arches, may also be disrupted.

Cardiac neural crest migrate to the outflow tract cushions

In order to determine whether cardiac neural crest-derived cells migrate into the pharyngeal arches and outflow tract in embryos with pulmonary atresia, we evaluated cyclopamine-treated quail-chick chimeras. By using the 0.8 μg/μl cyclopamine dose, which gave rise to a large percentage of PTA, we could also determine whether PTA was a primary neural crest defect or a secondary effect based on the initial secondary heart field defect. Quail-chick neural crest chimeras were treated with cyclopamine at HH 14 and incubated until HH 23-24, when cardiac neural crest-derived cells reach the outflow tract cushions. Quail cells were seen surrounding the arch arteries (data not shown). Quail cells also entered the outflow tract cushions and were seen in two distinct prongs (n=3, Fig. 8A, B). The two prongs were unequal in size, but the pattern was normal (Kirby et al., 1983). The quail neural crest-derived cells that entered the outflow tract were not dying, as indicated by an absence of TUNEL-positive quail cells. This result is consistent with the work of Lin et al. (2006), who showed that cardiac neural crest-derived cells migrate into the outflow tract in conditional knockouts that eliminated hedgehog signaling from Isl-1 expressing cells.

Interestingly, the cardiac neural crest-derived cells form an outflow tract septum but do not symmetrically divide the outflow tract after cyclopamine treatment (Fig. 8D, F). After septation is complete, the septum formed closer to the pulmonary side of the arterial trunk in cyclopamine-treated chimeras (n=2). The identity of the aorta was also confirmed by the presence of coronary arteries, which arose from the aortic wall. The presence of cardiac neural crest-derived cells indicates that pulmonary atresia is not associated with a failure of outflow tract septation. No chimeras were observed with PTA, precluding the possibility of determining whether the cardiac neural crest are present in the outflow tract in PTA associated with cyclopamine treatment. Together, these results show that cardiac neural crest migration and survival are not affected by hedgehog signaling between HH 14 and HH 18 and suggest that the sixth aortic arch artery abnormalities may instead be caused by direct effects of hedgehog signaling on the pharyngeal arches. Increased apoptosis observed in the caudal arches at HH 16, when neural crest cells have not yet populated the sixth pharyngeal arch, supports this hypothesis (Supplementary Figure 2).

Discussion

Shh-null mice exhibit extensive defects (Lititung et al., 1998; Tsukui et al., 1999; Chiang et al., 2001), and the heart displays a broad range of malformations, including pulmonary atresia, atrial and ventricular septal defects, and atrioventricular valve defects (Washington-Smoak et al., 2005). Tissue-specific knockout mice have shown that the pharyngeal endoderm is the critical source of Shh for heart development (Goddeeris et al., 2007), but even in these mice, the cardiac neural crest cells die in the pharyngeal arches. This additional defect complicates the issue of how Shh can affect a discrete population of cells, such as the secondary heart field, independent of other populations, such as the cardiac neural crest.

The present study avoids many other defects by inhibiting hedgehog signaling in a temporally discrete fashion. While application of hedgehog inhibitor cyclopamine was performed globally, it has a short period of activity (less than 24 hours), reducing its ability to influence other aspects of heart development. Few defects were found outside of the heart, and heart defects were limited to the arterial pole. Blocking hedgehog signaling in secondary heart field explants slightly reduced migration and dramatically reduced proliferation. By applying cyclopamine in ovo at the onset of the myocardial contribution from the secondary heart field to the outflow tract, we showed that the arterial pole defects were linked to a localized decrease in secondary heart field proliferation. Blocking Shh after the myocardium has been added to the outflow tract (HH 18) resulted in normal heart development. Because inhibiting this signaling pathway has such a pronounced effect, the timing of Shh signaling must be critical and tightly regulated in order to maintain the correct rate of proliferation and migration.

The secondary heart field remains a pool of undifferentiated progenitors until these cells migrate into the outflow tract and differentiate (Waldo et al., 2001). Nkx2.5 and Isl1 demarcate the initial bilateral heart field, and continued expression of these markers is associated with the pool of proliferative progenitors (Prall et al., 2007 and Cai et al., 2003). Additionally, Isl1 induces Shh expression in the pharyngeal endoderm (Lin et al, 2006) and proliferation in the splanchnic mesoderm of the second heart field (Cai et al., 2003). Eliminating the downstream signaling component Smoothened (Smo) from Isl1-positive cells causes PTA and pharyngeal arch patterning defects (Lin et al., 2006), both of which are seen after cyclopamine treatment in this study. β-catenin is also required for proliferation of Isl1-positive cardiac progenitors and may regulate Shh in the foregut endoderm (Lin et al., 2007). The overlapping signaling factors required to maintain proliferation must be tightly regulated because the secondary heart field fails to migrate into the arterial pole if too much (Waldo et al., 2005b) or too little (Xu et al., 2004 and this paper) proliferation occurs.

Shh is upstream of cell cycle genes that control both the G1-S transition, such as cyclins D1 and E (Kenney and Rowitch, 2000) and n-myc (Oliver et al., 2003), and the G2-M transition, such as CDC25B (Benezeraf et al., 2006). The effect of Shh on CDC25 is a non-cell autonomous effect, which is consistent with the finding that the secondary heart field can respond to Shh produced in the pharyngeal endoderm. Interestingly, Shh is incapable of recruiting quiescent neuronal cells into the cell cycle (Kenney and Rowitch, 2000). If Shh similarly cannot induce terminally differentiated cells to proliferate, this datum would suggest that Shh would only be able to maintain proliferation in non-differentiated myocardial precursors. Shh also defines the mitogenic niche for cerebellar granular cells (Choi et al., 2005); when neuronal precursors migrate away from the source of Shh, proliferation decreases. The caudal secondary heart field might serve as a niche that holds cells in a proliferative state until either they migrate into the outflow tract or the outflow tract is displaced caudally with respect to the pharyngeal arches and comes in close enough proximity to initiate a differentiation signaling cascade.

Interestingly, BMP2 is expressed in the outflow tract and promotes differentiation (Waldo et al, 2001). In addition, it specifically inhibits Shh-induced proliferation by down-regulating n-myc expression (Alvarez-Rodriguez et al, 2007), supporting the idea of a proliferative niche within the secondary heart field that is distinct from the migratory secondary heart field that is entering the outflow tract and in close proximity to BMP2.

Laser ablation of the right side of the secondary heart field, which physically reduces the number of cells that can contribute to the outflow tract, results in pulmonary stenosis and atresia (Ward et al., 2005). Reducing proliferation in the secondary heart field by applying cyclopamine could also result in fewer cells that can contribute to the arterial pole. Using a mouse Tbx1 hypomorph, Xu et al. (2004) showed that proliferation was reduced in the secondary heart field and suggested a correlation between secondary heart field proliferation and its myocardial contribution to the outflow tract. Like the cyclopamine-treated chick, this mouse mutant predominantly exhibits a single outflow vessel, and the pulmonary infundibulum is reduced in size; in some of these embryos, the single outflow vessel sits over the ventricular septal defect, but in others, this vessel arises predominantly from the left ventricle and looks more like an aorta than a common trunk (Théveniau-Ruissy et al, 2008). Cardiac neural crest-derived cells still migrate into the pharyngeal arches, although at reduced levels in the fourth arches. Our studies show that neural crest-derived quail cells still migrated into the outflow tract cushions of cyclopamine-treated chick embryos and formed a septum that was positioned incorrectly, effectively closing off the pulmonary outlet and resulting in pulmonary atresia.

In cyclopamine-treated embryos, pulmonary stenosis, pulmonary atresia, and PTA are all observed. There are a few ways that this range of defects can occur. The first is that the outflow tract myocardium produces signals that serve as a chemoattractant, encouraging the cardiac neural crest-derived cells to migrate into the cushions. Less myocardium would then secrete less chemoattractant and may only weakly attract the cardiac neural crest-derived cells. However, normal numbers of cardiac neural crest-derived cells were observed in the outflow tract cushions after hedgehog inhibition, making this possibility unlikely. Alternatively, intrinsic differences between aortic and pulmonary myocardium may set up a target for the cardiac neural crest-derived cells as they migrate into the outflow tract (Bajolle et al., 2008); a specific reduction in pulmonary myocardium would then result in the septum forming asymmetrically, as was observed in the present study. One could speculate that Shh has a left-right effect on the secondary heart field, similar to its earlier role as the first left-restricted gene during chick embryogenesis (Levin et al., 1997); a sided effect would explain why the pulmonary trunk was more severely affected.

Shh is upstream of left-restricted Pitx2c in the early lateral plate mesoderm (St. Amand et al., 1998), and Pitx2c is restricted to the left secondary heart field at E9.5 in mouse, which is at the end of the myocardial contribution (Liu et al., 2002). However, no other genes have been shown to have left-right asymmetry in the secondary heart field. Because the defects seen after cyclopamine treatment predominantly affect the pulmonary trunk, which is derived from the right side of the secondary heart field, it would be interesting to determine whether there is a right-sided transcription factor or signaling pathway that is altered after cyclopamine treatment. This possibility, though, does not address what causes PTA.

Because PTA, which is caused by a failure of cardiac neural crest-derived cells to septate the outflow tract, was favored in embryos treated with 0.8 μg/μl cyclopamine, quail-chick chimeras were treated with this dose in order to determine whether the cardiac neural crest was directly affected. However, cardiac neural crest-derived cells migrated into the pharyngeal arches and the outflow tract cushions and did not undergo apoptosis. Despite the predominant PTA phenotype observed with this cyclopamine dose, the cardiac neural crest cells migrate normally and survive. However, the cardiac neural crest-derived cells may not behave normally once

reaching the outflow tract. Another possibility is that not enough cardiac neural crest-derived cells populate the outflow tract, resulting in either a smaller septum that divides the outflow tract unequally or fails to septate the outflow tract at all.

The cyclopamine-induced defects seen after outflow tract septation occurs are likely caused by reducing the number of secondary heart field progenitors. This decrease results in both fewer myocardial and smooth muscle cells. The role of Shh in maintaining proliferation is critical, but other factors must contribute to this regulation. Further work will be necessary to tease apart the factors that control regional proliferation to better understand how the secondary heart field contributes to the arterial pole and how this contribution is miscued during heart malformations.

Supplementary Material

Refer to Web version on PubMed Central for supplementary material.

Acknowledgments

We would like to thank Drs. Mary Hutson and Adrian Grimes for advice and discussion, Harriett Stadt and Ping Zhang for technical assistance, Dr. Joe Lucas for statistical advice, and Dr. Cliff Tabin (Harvard University) for generously providing the Shh and Ptc2 plasmids.

References

Abu-Issa R, Smyth G, Smoak I, Yamamura K, Meyers EN. Fgf8 is required for pharyngeal arch and cardiovascular development in the mouse. Development 2002;129:4613–25. [PubMed: 12223417]

Allan GJ, Zannoni A, McKinnel I, Otto WR, Holzenberger M, Flint DJ, Patel K. Major components of the insulin-like growth factor axis are expressed early in chicken embryogenesis, with IGF binding protein (IGFBP)-5 expression subject to regulation by Sonic Hedgehog. Anat Embryol (Berl) 2003;207:73–84. [PubMed: 12743812]

Alvarez-Rodriguez R, Barzi M, Berenguer J, Pons S. Bone morphogenetic protein 2 opposes Shh-mediated proliferation in cerebellar granule cells through a TIEG-1-based regulation of Nmyc. J Biol Chem 2007;282:37170–37180. [PubMed: 17951258]

Arnold JS, Werling U, Braunstein EM, Liao J, Nowotschin S, Edelmann W, Hebert JM, Morrow BE. Inactivation of Tbx1 in the pharyngeal endoderm results in 22q11DS malformations. Development 2006;133:977–987. [PubMed: 16452092]

Bajolle F, Zaffran S, Meilhac SM, Dandonneau M, Chang T, Kelly RG, Buckingham ME. Myocardium at the base of the aorta and the pulmonary trunk is prefigured in the outflow tract of the heart and in subdomains of the second heart field. Dev Biol 2008;313:25–34. [PubMed: 18005956]

Benazeraf B, Chen Q, Peco E, Lobjois V, Medevielle F, Ducommun B, Pituello F. Identification of an unexpected link between the Shh pathway and a G2/M regulator, the phosphatase CDC25B. Dev Biol 2006;294:133–47. [PubMed: 16564519]

Bockman DE, Redmond ME, Waldo K, Davis H, Kirby ML. Effect of neural crest ablation on development of the heart and arch arteries in the chick. Am J Anat 1987;180:332–341. [PubMed: 3425561]

Cai CL, Liang X, Shi Y, Chu PH, Pfaff SL, Chen J, Evans S. Isl1 identifies a cardiac progenitor population that proliferates prior to differentiation and contributes a majority of cells to the heart. Dev Cell 2003;5:877–889. [PubMed: 14667410]

Choi Y, Borghesani PR, Chan JA, Segal RA. Migration from a mitogenic niche promotes cell-cycle exit. J Neurosci 2005;25:10437–10445. [PubMed: 16280582]

Epstein JA, Li J, Lang D, Chen F, Brown CB, Jin F, Lu MM, Thomas M, Liu E, Wessels A, et al. Migration of cardiac neural crest cells in Splotch embryos. Development 2000;127:1869–1878. [PubMed: 10751175]

Frank DU, Fotheringham LK, Brewer JA, Muglia LJ, Tristani-Firouzi M, Capecchi MR, Moon AM. Development 2002;129:4591–603. [PubMed: 12223415]

Fu M, Lui VCH, Sham MH, Pachnis V, Tam PKH. Sonic hedgehog regulates the proliferation, differentiation, and migration of enteric neural crest cells in gut. J Cell Biol 2004;166:673–684. [PubMed: 15337776]

Garg V, Yamagishi C, Hu T, Kathiriya IS, Yamagishi H, Srivastava D. Tbx1, a DiGeorge syndrome candidate gene, is regulated by Sonic hedgehog during pharyngeal arch development. Dev Biol 2001;235:62–73. [PubMed: 11412027]

Goddeeris MM, Schwartz R, Klingensmith J, Meyers EN. Independent requirements for Hedgehog signaling by both the anterior heart field and neural crest cells for outflow tract development. Development 2007;134:1593–1604. [PubMed: 17344228]

Hamburger V, Hamilton H. Series of Embryonic Chicken Growth. J Morphol 1951;88:49–92.

Hiruma T, Hirakow R. Formation of the pharyngeal arch arteries in the chick embryo. Observations of corrosion casts by scanning electron microscopy. Anat Embryol (Berl) 1995;191:415–423. [PubMed: 7625612]

Hoffman JI, Kaplan S. The incidence of congenital heart disease. J Am Coll Cardiol 2002;39:1890–1900. [PubMed: 12084585]

Hutson MR, Zhang P, Stadt HA, Sato AK, Li YX, Burch J, Creazzo TL, Kirby ML. Cardiac arterial pole alignment is sensitive to FGF8 signaling in the pharynx. Dev Biol 2006;295:486–497. [PubMed: 16765936]

Ingham PW, McMahon AP. Hedgehog signaling in animal development: paradigms and pinrciples. Genes Dev 2001;15:3059–3087. [PubMed: 11731473]

Jarov A, Williams KP, Ling LE, Koteliansky VE, Duband JL, Fournier-Thibault C. A dual role for Sonic hedgehog in regulating adhesion and differentiation of neuroepithelial cells. Dev Biol 2003;261:520–536. [PubMed: 14499657]

Jones RG, Li X, Gray PD, Kuang J, Clayton F, Samowitz WS, Madison BB, Gumucio DL, Kuwada SK. Conditional deletion of beta-1 integrins in the intestinal epithelium causes a loss of hedgehog expression, intestinal hyperplasia, and early postnatal lethality. J Cell Biol 2006;175:505–514. [PubMed: 17088430]

Kenney AM, Rowitch DH. Sonic hedgehog promotes G(1) cyclin expression and sustained cell cycle progression in mammalian neuronal precursors. Mol Cell Biol 2000;20:9055–9067. [PubMed: 11074003]

Kirby ML, Gale TF, Steward DE. Neural crest cells contribute to normal aorticopulmonary septation. Science 1983;220:1059–1061. [PubMed: 6844926]

Kirby ML. Nodose placode contributes autonomic neurons to the heart in the absence of cardiac neural crest. J Neurosci 1988;10:1089–1095. [PubMed: 3357010]

Kirby, ML. Cardiac Development. Oxford: Oxford University Press; 2007.

Levin M, Pagan S, Roberts DJ, Cooke J, Kuehn MR, Tabin CJ. Left/right patterning signals and the independent regulation of different aspects of situs in the chick embryo. Dev Biol 1997;189:57–67. [PubMed: 9281337]

Lin L, Bu L, Cai CL, Zhang X, Evans S. Isl1 is upstream of sonic hedgehog in a pathway required for cardiac morphogenesis. Dev Biol 2006;295:756–763. [PubMed: 16687132]

Lin L, Cui L, Zhou W, Dufort D, Zhang X, Cai CL, Bu L, Yang L, Martin J, Kemler R, et al. Beta-catenin directly regulates Islet1 expression in cardiovascular progenitors and is required for multiple aspects of cardiogenesis. P Natl Acad Sci USA 2007;104:9313–9318.

Moore-Scott B, Manley N. Differential expression of Sonic hedgehog along the anterior–posterior axis regulates patterning of pharyngeal pouch endoderm and pharyngeal endoderm-derived organs. Dev Biol 2005;278:323–335. [PubMed: 15680353]

Oliver TG, Grasfeder LL, Carroll AL, Kaiser C, Gillingham CL, Lin SM, Wickramasinghe R, Scott MP, Wechsler-Reya RJ. Transcriptional profiling of the Sonic hedgehog response: a critical role for N-myc in proliferation of neuronal precursors. P Natl Acad Sci USA 2003;100:7331–7336.

Pfaffl, MW. Quantification strategies in real-time PCR. In: Bustin, SA., editor. A-Z of quantitative PCR. International University Line; La Jolla, CA: 2004. p. 87-120.

Prall OW, Menon MK, Solloway MJ, Watanabe Y, Zaffran S, Bajolle F, Biben C, McBride JJ, Roberston BR, Chaulet H, et al. An Nkx2-5/Bmp2/Smad1 negative feedback loop controls heart progenitor specification and proliferation. Cell 2007;128:947–959. [PubMed: 17350578]

Rosamond W, Flegal K, Friday G, Furie K, Go A, Greenlund K, Haase N, Ho M, Howard V, Kissela B, et al. Heart disease and stroke statistics--2007 update: a report from the American Heart Association Statistics Committee and Stroke Statistics Subcommittee. Circulation 2007;115:e69–e171. [PubMed: 17194875]

St Amand TR, Ra J, Zhang Y, Hu Y, Baber SI, Qiu MS, Chen YP. Cloning and expression pattern of chicken Pitx2: a new component in the Shh signaling pathway controlling embryonic heart looping. Biochem Bioph Res Co 1998;247:100–105.

Testaz S, Jarov A, Williams KP, Ling LE, Koteliansky VE, Fournier-Thibault C, Duband JL. Sonic hedgehog restricts adhesion and migration of neural crest cells independently of the Patched-Smoothened-Gli signaling pathway. P Natl Acad Sci USA 2001;98:12521–12526.

Théveniau-Ruissy M, Dandonneau M, Mesbah K, Glez O, Mattei MG, Miquerol L, Kelly RG. The del22q11.2 candidate gene Tbx1 controls regional outflow tract identity and coronary artery patterning. Circ Res 2008;18:142–148.

Waldo KL, Kumiski D, Kirby ML. Cardiac neural crest is essential for the persistence rather than the formation of an arch artery. Dev Dynam 1996;205:281–292.

Waldo KL, Miyagawa-Tomita S, Kumiski D, Kirby ML. Cardiac neural crest cells provide new insight into septation of the cardiac outflow tract: aortic sac to ventricular septal closure. Dev Biol 1998;196:129–144. [PubMed: 9576827]

Waldo KL, Kumiski DH, Wallis KT, Stadt HA, Hutson MR, Platt DH, Kirby ML. Conotruncal myocardium arises from a secondary heart field. Development 2001;128:3179–3188. [PubMed: 11688566]

Waldo KL, Hutson MR, Stadt HA, Zdanowicz M, Zdanowicz J, Kirby ML. Cardiac neural crest is necessary for normal addition of the myocardium to the arterial pole from the secondary heart field. Dev Biol 2005a;281:66–77. [PubMed: 15848389]

Waldo KL, Hutson MR, Ward CC, Zdanowicz M, Stadt HA, Kumiski D, Abu-Issa R, Kirby ML. Secondary heart field contriubtes myocardium and smooth muscle to the arterial pole of the developing heart. Dev Biol 2005b;281:78–90. [PubMed: 15848390]

Ward CC, Stadt HA, Hutson MR, Kirby ML. Ablation of the secondary heart field leads to tetralogy of fallot and pulmonary atresia. Dev Biol 2005;284:72–83. [PubMed: 15950213]

Washington Smoak I, Byrd NA, Abu-Issa R, Goddeeris MM, Anderson R, Morris J, Yamamura K, Klingensmith J, Meyers EN. Sonic hedgehog is required for cardiac outflow tract and neural crest cell development. Dev Biol 2005;283:357–372. [PubMed: 15936751]

Wilkinson, DG. In Situ Hybridization: A Practical Approach. Oxford: IRS Press; 1992.

Williams JM, de Leeuw M, Black MD, Freedom RM, Williams WG, McCrindle BW. Factors associated with outcomes of persistent truncus ateriosus. J Am Coll Cardiol 1999;34:545–553. [PubMed: 10440171]

Xu H, Morishima M, Wylier JN, Schwartz RJ, Bruneau BG, Lindsay EA, Baldini A. Tbx1 has a dual role in the morphogenesis of the cardiac outflow tract. Development 2004;131:3217–3227. [PubMed: 15175244]

Yelbuz TM, Waldo KL, Kumiski D, Stadt HA, Wolfe RR, Leatherbury L, Kirby ML. Shortened outflow tract leads to altered cardiac looping after neural crest ablation. Circulation 2002;106:504–510. [PubMed: 12135953]

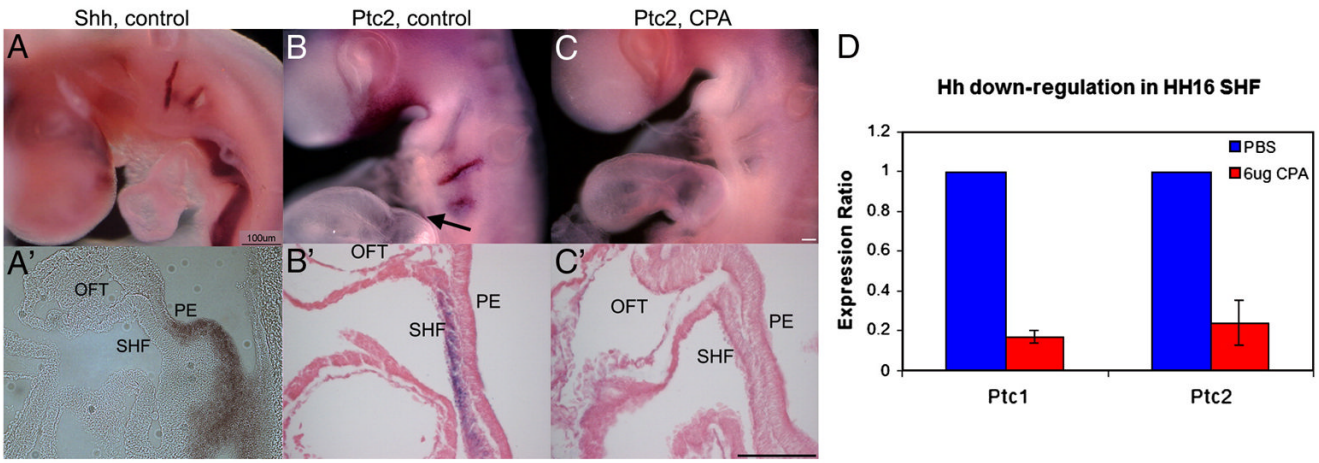

Figure 1.

Expression of hedgehog signaling components during secondary heart field (SHF) development in chick embryos. (A, A′) Shh in situ hybridization at HH 15 shows expression in pharyngeal clefts 2 and 3 and the foregut (A), specifically the pharyngeal endoderm (PE, A ′). (B, B′) Ptc2 in situ hybridization at HH 16 shows a similar wholemount pattern (B); however, Ptc2 is restricted to the SHF mesoderm adjacent to the Shh-expressing endoderm. (C, C′) Within 12 hours, cyclopamine (CPA)-treated embryos show no expression of receptor and downstream target Ptc2, as observed by in situ hybridization. Embryos were treated at HH 14 and collected at HH 16. Ptc2 expression is absent after CPA treatment. Time allowed for color development was the same for embryos in both B and C. (D) Quantitative RT-PCR was used to analyze isolated SHF from HH 16 embryos. Both Ptc1 and Ptc2 are significantly down-regulated after CPA treatment ($p<0.01$ for both). Scale bar in C is 100 μm in A–C, and the scale bar in C′ is 200 μm in A′ and 100 μm in B′–C′; OFT, outflow tract. Scale bar in B is 100 μm and applies to A; scale bar in D is 100 μm and applies to C.

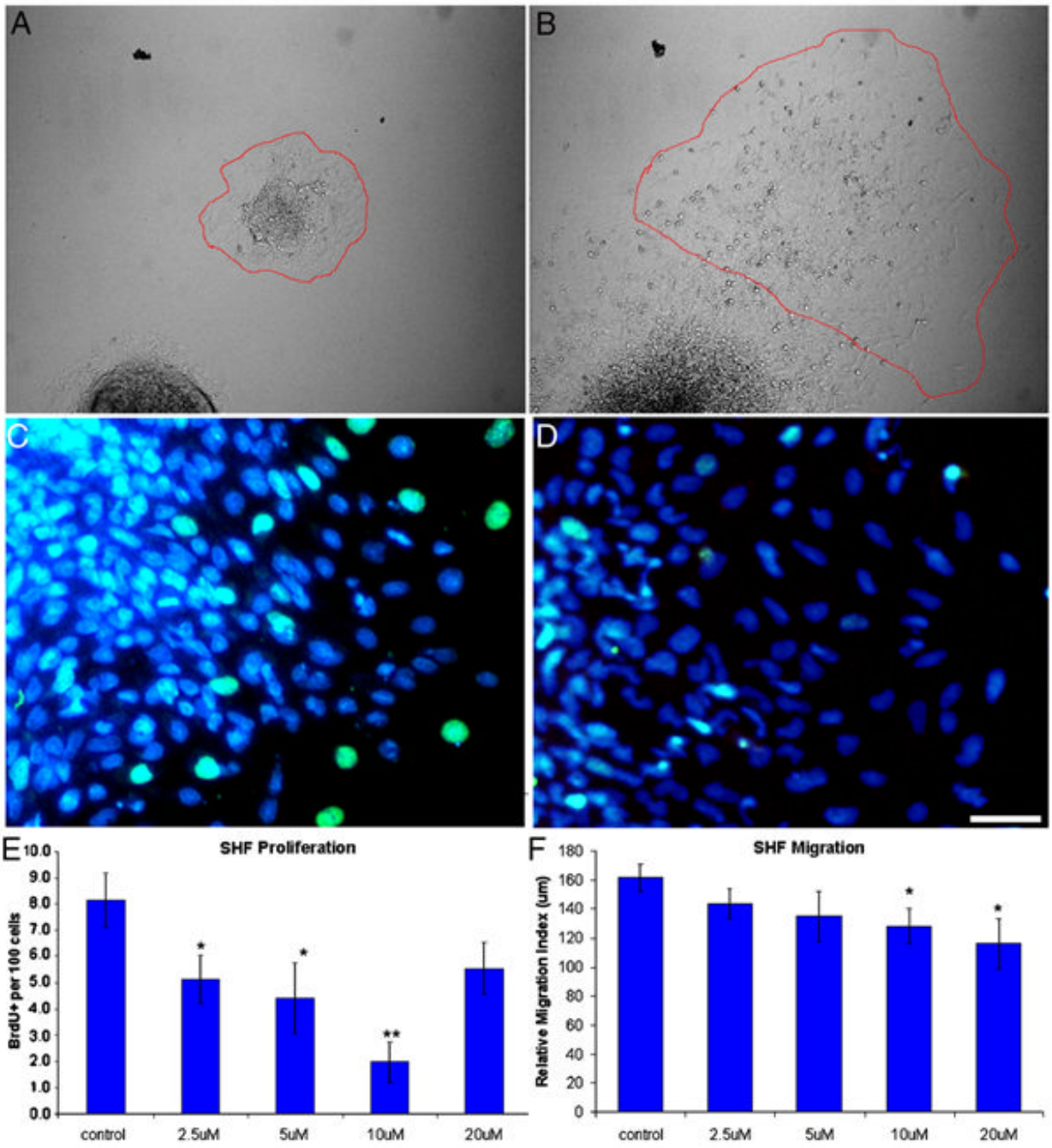

Figure 2.

Cyclopamine (CPA) reduces proliferation and migration in vitro. (A) Before and (B) after images of a control explant during the 16-hour migration assay. The perimeter of the explant is highlighted in red. (C, D) Explants were treated with PBS (C) or CPA (D) and labeled with BrdU (green) and DAPI (blue). Note the reduction of BrdU-positive secondary heart field (SHF) mesoderm after CPA treatment. (E) Treating SHF explants with CPA reduces proliferation after 24 hours. (F) Treating SHF explants with CPA reduces migration over a 16-hour period. The highest dose reversed the anti-proliferative effect, suggesting a narrow range of anti-proliferative signaling. Scale bar is 25 μm in A and B. *$p \leq 0.05$, **$p \leq 0.0001$

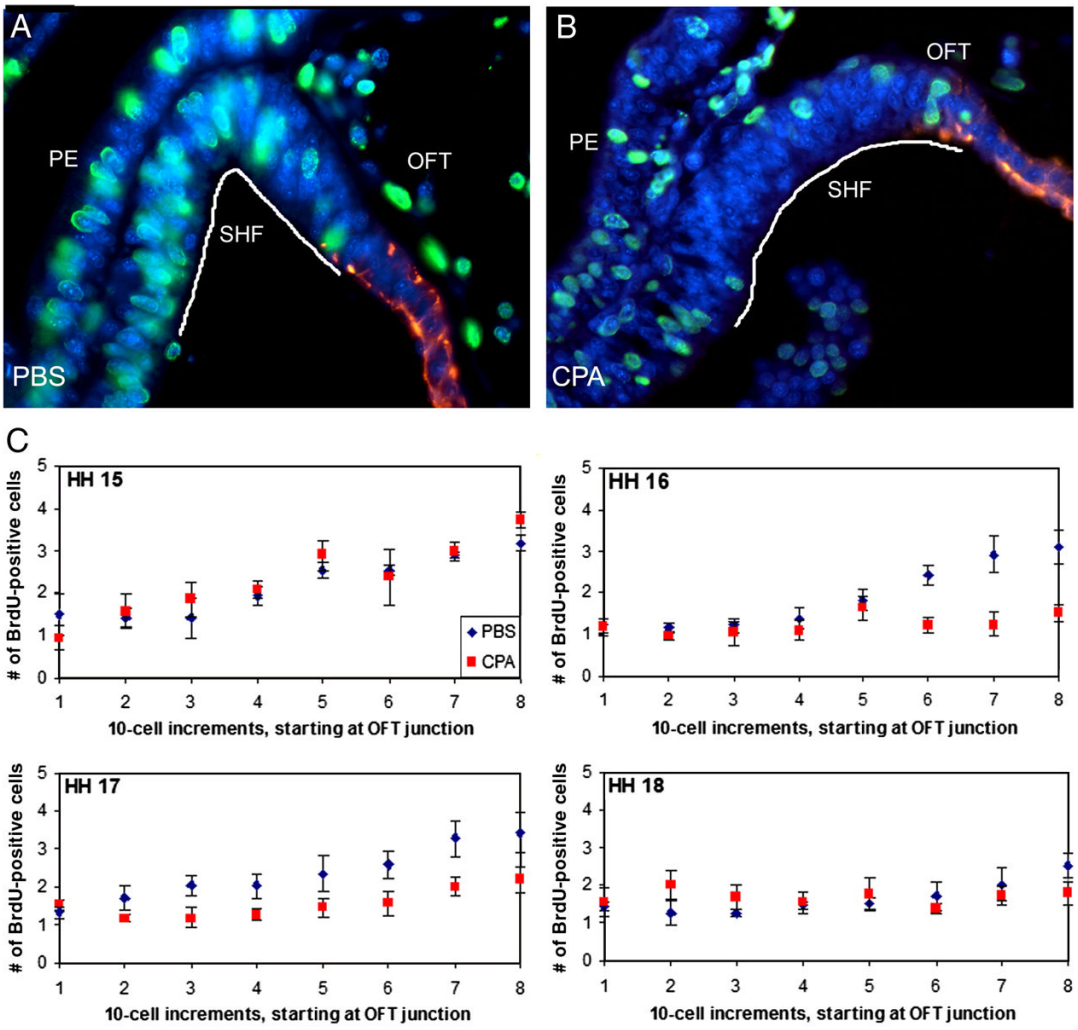

Figure 3.

Cyclopamine (CPA) treatment disrupts secondary heart field (SHF) proliferation in ovo. (A) HH 16 control embryo and (B) HH 16 embryo treated with 0.6 μg/μl CPA at HH 14. Embryos were labeled with BrdU (green nuclei) at HH 16; myocardium is red. (C) Total BrdU-positive cells counted in 10-cell increments at HH 15 to 18. SHF cells were counted starting at the myocardial border of the outflow tract (OFT; increment 1), as delineated with a myocardial marker (red) in (A) and (B), and moving caudally through the splanchnic mesoderm (with increment 8 being the most caudal). Between HH 15 and 17, proliferation in the SHF adjacent to the pharyngeal endoderm (the caudal-most 30 cells) occurs at nearly twice the rate that is seen in the 50 cranial-most cells. Within 12 hours of cyclopamine treatment (HH 16), proliferation is no longer increased in the caudal SHF ($p<0.01$ for increments 6–8); this decrease is maintained through HH 17 ($p<0.05$ for increments 6–8). By HH 18, no differences are observed in CPA-treated embryos compared to control embryos. Scale bar is 100 μm.

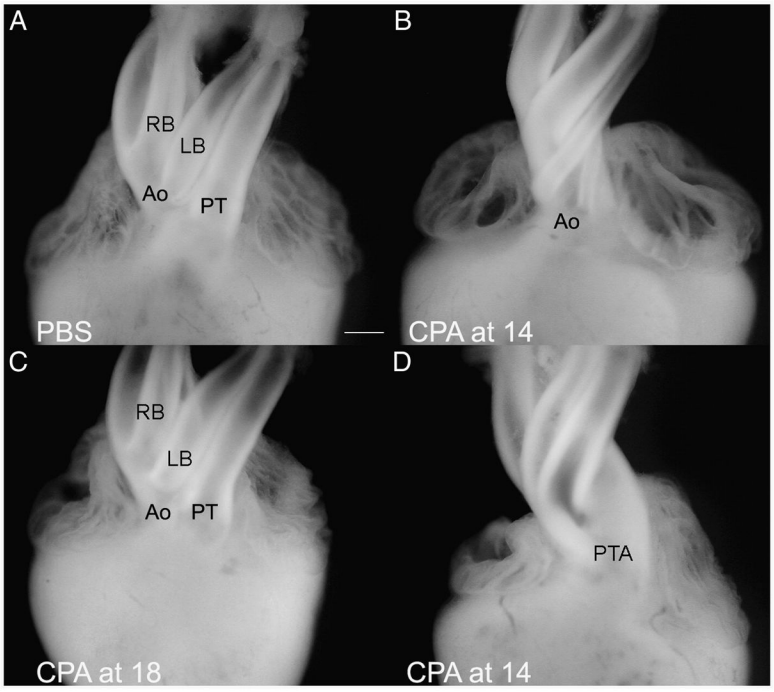

Figure 4.

Cyclopamine (CPA) treatment induces arterial pole defects. (A) PBS-treated control; (B), (D), hearts treated with 0.6 μg/μl CPA at HH 14; (C) heart treated with 1.0 μg/μl CPA at HH 18. Embryos treated at HH 14 show a range of defects, but all have a single outflow vessel, and the origins of the great arch arteries are shifted to the right side and originate more proximal to the ventricles. Histological analysis identified the single vessel. The single vessel in (B) is an Ao (Ao); the single vessel in (D) is persistent truncus arteriosus (PTA). Embryos treated at HH 18 (C) are morphologically indistinguishable from controls. PT, pulmonary trunk; RB, right brachiocephalic; LB, left brachiocephalic. Scale bar is 175 μm.

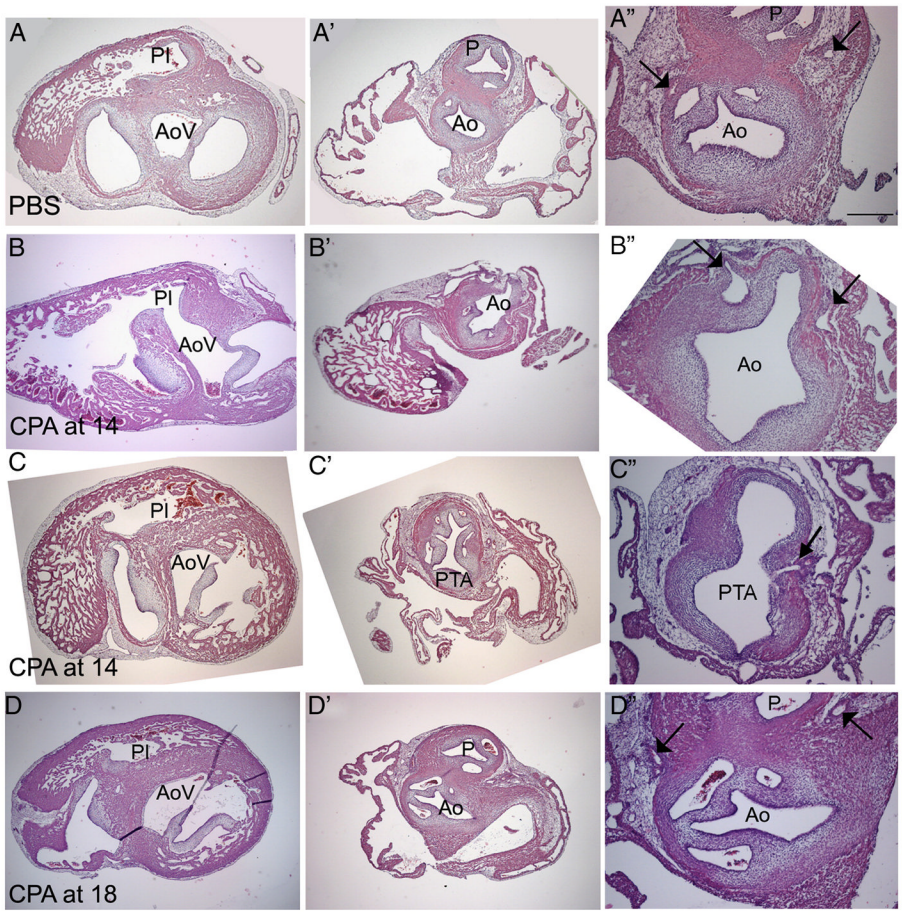

Figure 5.

Histological analysis of HH 35 hearts. (A–A″) PBS-treated control; (B–B″; C–C″) heart treated with 0.6 μg/μl CPA at HH 14; (D–D″) heart treated with 1.0 μg/μl at HH 18. In the control heart (A), the aortic vestibule (AoV) and pulmonary infundibulum (PI) are separated (A) and about the same size. At the valve level, two robust arterial trunks can be seen in the correct orientation. The aorta (Ao) is identified based on its origin from the AoV (A), its posterior position relative to the pulmonary artery (P) at the valve level (A″), and the presence and position of two coronary artery stems from the coronary sinuses (arrows in A″). After CPA treatment at HH 14 (B), a ventricular septal defect allows a connection between the small PI and the AoV (B). The PI disappears before reaching the single outflow vessel (B″). The presence of two coronary arteries penetrating the single outflow vessel further confirms the identity of the Ao (arrows in B″), indicating that this embryo had pulmonary atresia. Another embryo treated at HH 14 (C) exhibits pulmonary atresia. While a ventricular septal defect is present, this defect is very high. The single outflow vessel has five valve leaflets (C″); in addition, two coronary arteries penetrate the aortic side of the single outflow vessel, one of which is seen in C″ (arrow). Treatment at HH 18 (D) results in a well-formed ventricular septum (D), divided arterial valves, (D″) and normal coronary arteries (arrows in D″). Scale bar is 250 μm in A–A″ and 100 μmin A″; the same scales apply to rows B–D.

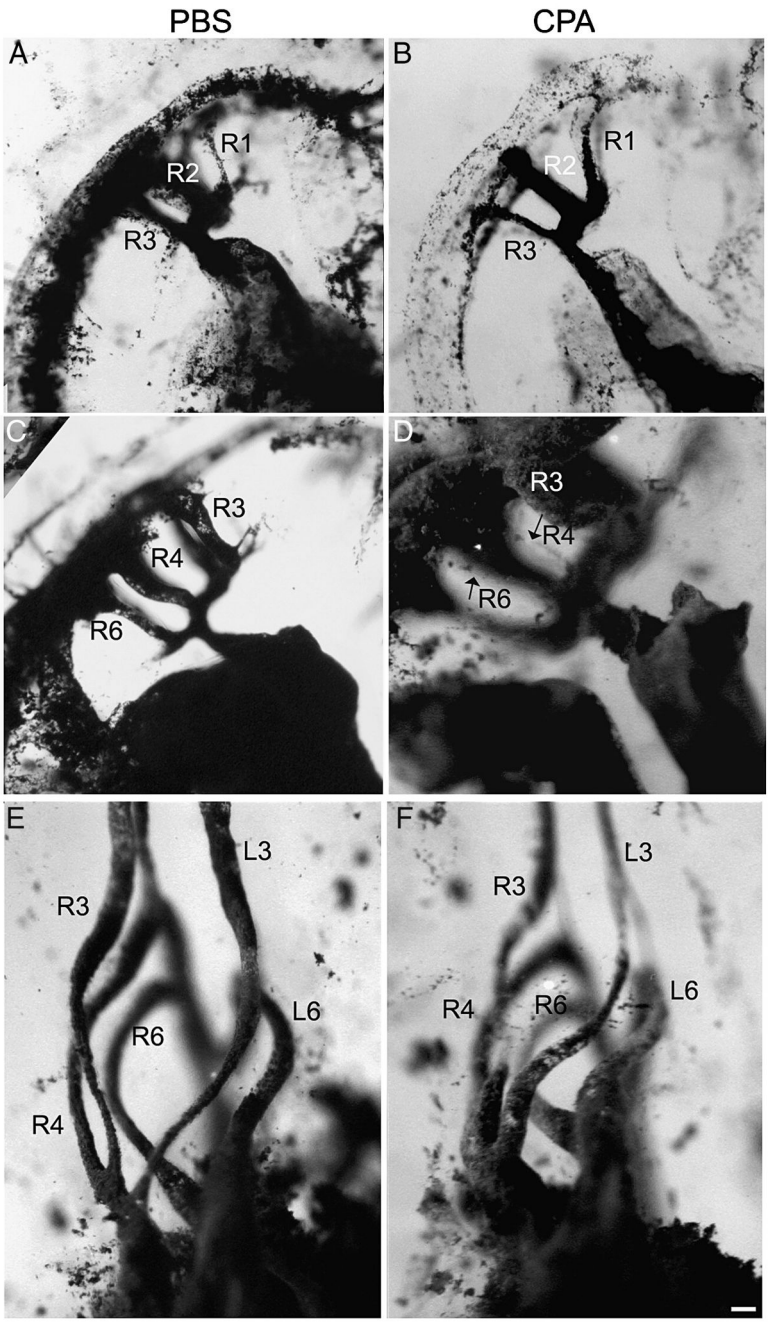

Figure 6.

India ink injections of PBS- (A, C, E) and cyclopamine (CPA)-treated (B, D, F) embryos. CPA-treated embryos at HH 18 (B) have a persistent first arch artery, compared to the control (A), where it has begun to regress. In addition, the junction between the aortic sac and the outflow tract is widened after CPA treatment. By stage HH 22-23, arch arteries 3, 4, and 6 are normally open (C); however, after CPA treatment, pharyngeal arch arteries 4 and 6 are very small (thin endothelial strands marked with arrows in D). Right arch arteries 4 and 6 are so thin that the left arch arteries are visible, unlike in the control. At HH 29, the appropriate pharyngeal arch arteries appear to be present (compare cyclopamine-treated F with control E). Arch arteries are labeled according to arch number and side. Scale bar is 100 μm.

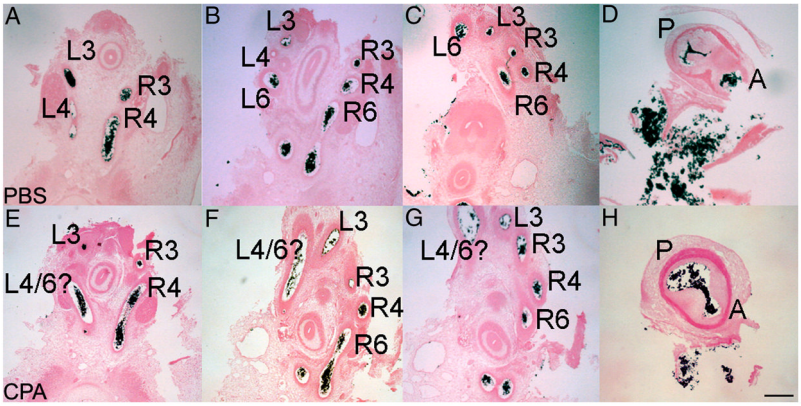

Figure 7.

Sectioned India ink-injected embryos at HH 29. A–D, PBS-treated embryo; EH, CPA-treated embryo. In the control, the left fourth arch artery (L4) is regressing (B), and a septum is beginning to divide the outflow tract (D). In the CPA-treated embryo, the left 4/6 arch artery (L4/6) is not at the level of either the fourth or sixth arch (E–F), and an open communication persists between the pulmonary (P) and aortic (A) trunks (arrow, H). Arch arteries are labeled according to arch number and side. Scale bar is 200 μm.

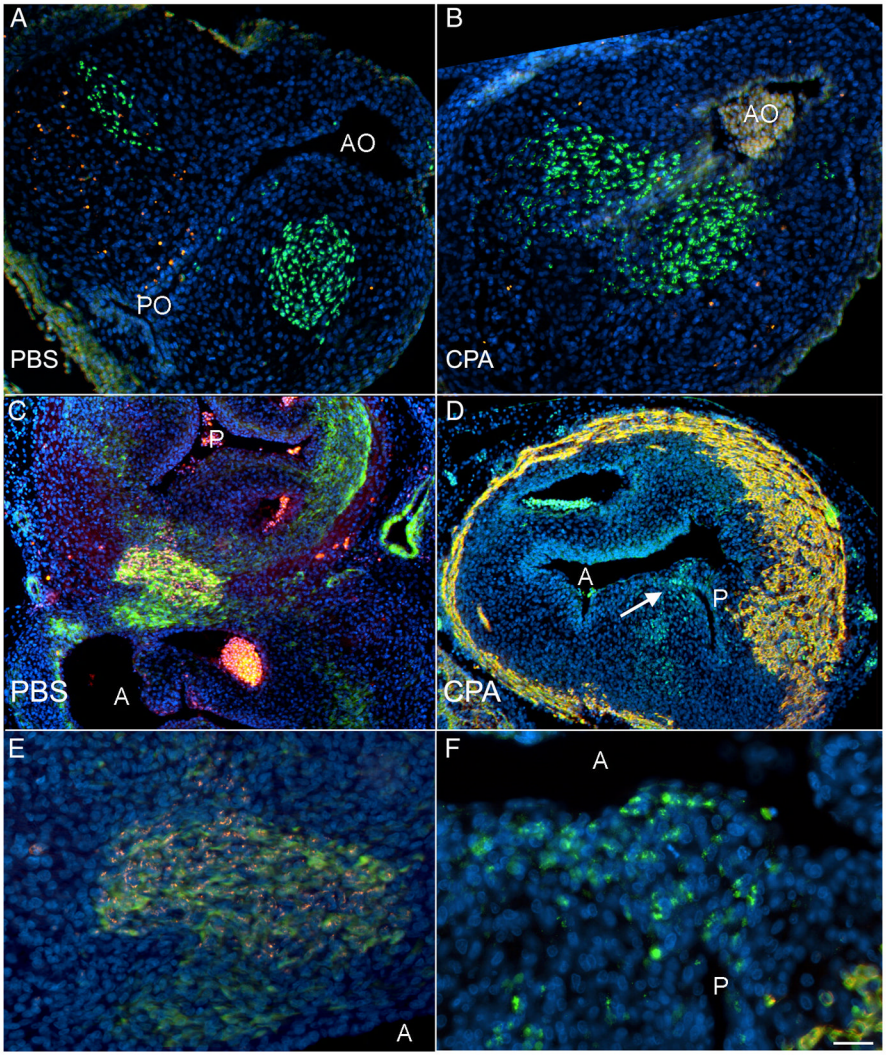

Figure 8.

Quail-chick chimeras treated with PBS (A, C, E) and cyclopamine (CPA, B, D, F) show that the cardiac neural crest enter and septate the outflow tract (OFT). Apoptosis was analyzed before septation (HH 23-24, A, B). In both control (A) and cyclopamine-treated (B) chimeras, the quail neural crest-derived cells (green) are not TUNEL-positive (red) as they enter the OFT, indicating that these cells are not undergoing apoptosis. Nuclei are counterstained with DAPI (blue). Of note, the aortic outlet (AO) is open in both control (A) and CPA-treated (B) embryos; the pulmonary outlet (PO), though, is only open in the control embryo (A). After septation occurs (HH 35, C–F), the presence of quail neural crest-derived cells in the outflow tract was confirmed (red in C and close-up E; green in D and close-up F), and embryos were co-labeled with either myocardial marker MF20 (red in D and F) or smooth muscle marker SM22-α (green in C and E). Quail neural crest-derived cells are still present after CPA treatment (D); however, these cells do not form two equal-sized outflow vessels as seen in the control (C). Instead, the prominent outflow vessel in the CPA-treated chimera is the aorta (A), as determined by connection to the ventricles and the presence of a coronary artery; a small pulmonary (P) is septated by the quail neural crest-derived cells (highlighted with an arrow in D). The close-ups in E and F suggest that there may be a cell size difference after CPA treatment. C–F are co-labeled with DAPI. Scale bar is 100 μmin A–D and 50 μm in E–F.

Table 1

Quantitative RT-PCR primers

Gene	Primers	Size (bp)	Efficiency
Ptc1	Forward: 5′ AAGTGTAGCCCTTACATCTATCAG 3′ Reverse: 5′ CAACTGCTGCTTGGAGTG 3′	100	2.05
Ptc2	Forward: 5′ CTTCTACAGCCCTTGCTC 3′ Reverse: 5′ GGCATGGTTGTCGTTGG 3′	75	2.26
HPRT	Forward: 5′ CTGTAATGATCAGTCAACTGGA 3′ Reverse: 5′ ACCAACAAACTGGCCAC 3′	179	1.91

Table 2

Embryos treated at HH 14 with either dose of cyclopamine were significantly different from control embryos ($p=2.4\times10^{-8}$) and each other ($p=0.04$), as determined with Fisher's exact test.

Phenotype	Control (n=13)	0.6 μg/μl CPA (n=16)	0.8 μg/μl CPA (n=14)
Hypoplastic pulmonary infundibulum*	0	3	1
Atretic pulmonary outlet*	0	6	3
Stenotic pulmonary ouetlet	0	2	0
Persistent truncus arteriosus	0	2	6
Unidentifiable single outlet	0	1	1
Normal	13	2	3

* Both of these phenotypes were classified as pulmonary atresia based on the absence of a pulmonary artery.